

## **Elastic orange emissive single crystals of 1,3-diamino-2,4,5,6-tetrabromobenzene as flexible optical waveguides**

Venkatesh Gude,<sup>a</sup> Priyanka S. Choubey,<sup>b</sup> Susobhan Das,<sup>c</sup> Shivakiran Bhaktha B. N.,<sup>b,d</sup> C. Malla Reddy<sup>\*c</sup> and Kumar Biradha<sup>\*a</sup>

<sup>a</sup> Department of Chemistry, <sup>b</sup> School of Nano-Science and Technology, <sup>d</sup> Department of Physics, Indian Institute of Technology-Kharagpur, Kharagpur, West Bengal, 721302, India.

<sup>c</sup> Department of Chemical Sciences, Indian Institute of Science Education and Research-Kolkata, Nadia, West Bengal, 741246, India.

E-mail: [kbiradha@chem.iitkgp.ernet.in](mailto:kbiradha@chem.iitkgp.ernet.in), [cmallareddy@gmail.com](mailto:cmallareddy@gmail.com)

## Table of contents

	Description	Page No
	Experimental details and synthesis of compound 1	3
Fig. S1	Calculation of Elastic Strain	8
Table S1	Crystallographic parameters of compound 1	8
Fig. S2	An overlay of experimental and simulated powder X-ray diffraction pattern of compound 1	9
Fig. S3	DSC thermogram of compound 1	9
Fig. S4	QTAIM topology map to determine the halogen and hydrogen bond energies.	10
Fig. S5	(a) Absorption and (b) emission spectra at 320 nm excitation of compound 1 in a range of non-polar to polar solvents.	11
Fig. S6	Comparison of experimental absorption spectrum with the computed absorption spectrum at PBEPBE and DZVP level of theory. Excitation spectra of compound 1.	11
Fig. S7	The computed vertical excitation energies (VEEs) of compound 1 and nature transition orbitals (Iso value = 0.02) corresponding to various excited singlet states in vacuum at PBEPBE and DZVP level of theory.	12
Fig. S8	The computed vertical excitation energies (VEEs) of compound 1 and nature transition orbitals (Iso value = 0.02) corresponding to various excited singlet states in DCM at PBEPBE and DZVP level of theory.	13
Fig. S9	Emission spectra of compound 1 crystal in (a) unbent (b) bent shape and (c) solid state.	13
Table S2	Photo-physical parameters of compound 1	14
Table S3	The reported optical loss coefficient ( $\alpha$ ) of few organic single crystals and representative polymers.	14
	References	16

## **Experimental details and synthesis of compound 1:**

### **Experimental section:**

The diffuse reflectance spectrum (DRS) was recorded with a Cary model 5000 UV–vis-NIR spectrophotometer and the solid/solution state fluorescence spectra were recorded using a HORIBA Jobin Yvon-spex Fluorolog-3 spectrofluorimeter at room temperature.

Powder X-ray diffraction (PXRD) data of compound **1** was recorded with a BRUKER-AXS-D8-ADVANCE diffractometer (Cu K $\alpha$ ,  $\lambda$  = 1.5406 Å) at room temperature. Differential Scanning Calorimetry (DSC) thermogram recorded using model no. TA DSC Q20 equipment with the heating rate of 5 °C/min.

Single crystal x-ray diffraction data were collected on a Bruker-APEX-II CCD X-ray diffractometer that uses graphite monochromated Mo K $\alpha$  radiation ( $\lambda$  = 0.71073 Å) at 296 K by the hemisphere method. The structures were solved by direct methods and refined by least-squares methods on F<sup>2</sup> using SHELX-2014.<sup>1</sup> Non-hydrogen atoms were refined anisotropically, and hydrogen atoms were fixed at calculated positions and refined using a riding model.

Fluorescence lifetime measurements in ps-ns time domain were carried out using a time correlated single photon counting (TCSPC) spectrometer (Horiba, Fluorohub, Deltadiode). Diode laser with  $\lambda_{\text{ex}}$  = 485 nm was used as the excitation source. Instrument response function (IRF) was recorded using a scatterer (dilute solution of ludox in water). Nonlinear least squares iterative reconvolution procedure was employed to fit the fluorescence decay curve using a single/biexponential decay equation. The quality of the fit was assessed from the  $\chi^2$  values and the distribution of the residuals.

Halogen/hydrogen bond energies were calculated through quantum theory of atoms-in-molecules (QTAIM) approach; electrostatic potential (ESP) coloured molecular van der Waals (vdW) surface map (Iso value = 0.001) was computed using ‘Multiwfn’ analyzer at DZVP level of theory with PBEPBE functional. All the calculations were carried out using the Gaussian 09 package.<sup>2</sup> The vertical excitation energies and nature transition orbitals (NTOs) of compound **1** were calculated from the ground state optimized geometry with PBEPBE functional at DZVP level of theory using the TDDFT method in vacuum, dichloromethane and methanol (IEF-PCM model).

### **Nanoindentation experiments:**

The needle shaped single crystals of compound **1** were mounted on a coverslip using a small amount of adhesive liquid such as Fevi kwik. This coverslip was further fixed on top of a steel stub using the same adhesive to avoid the translational motion during experimentation.

The full details of experimental setup can be found in our previous reports.<sup>3,4</sup> In brief, nanoindentation experiments have been performed using Hysitron Triboindenter, TI Premier, Minneapolis, USA equipped with an in-situ Scanning Probe Microscope (SPM) employing a Berkovich tip having an effective radius of 150 nm.

## Optical waveguide experiments:

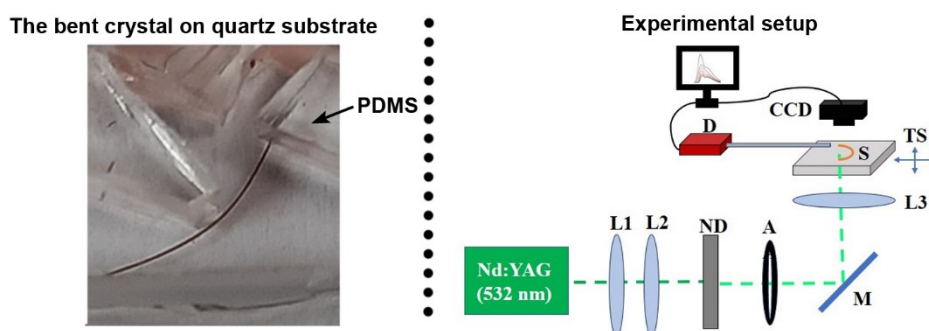
### PDMS mount preparation:

In order to mount the bent crystal, polydimethylsiloxane (PDMS) sheets were fabricated. PDMS pre-polymer and curing agent (Sylgard 184) were mixed thoroughly in 10:1 ratio and poured into a petri dish. The formed air bubbles were removed by degasification of the mixture. Later, the mixture was cured at 70 °C for 3 hr. The thin sheet ( $\approx 4$  mm thick) of PDMS was peeled off from a petri dish and a V-shaped cut was made carefully with a paper cutter. The PDMS sheet with V-shaped cut was then stuck to the Quartz substrate by plasma treatment using an air plasma setup (Omicron Scientific Equipment Co., India). The crystal was then carefully placed inside a V-shaped cut to mount the bent crystal with the help of a tweezer (see the provided image below).

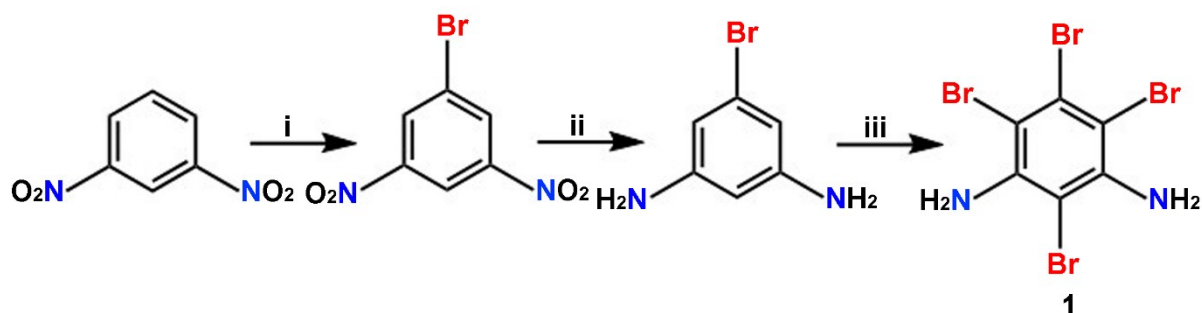
### Experimental setup:

In order to investigate the potential of fluorescent elastic crystals, the optical waveguide experiments have been performed in both the straight (unbent) and bent shape of crystal. The sample was irradiated by the second harmonic ( $\lambda_{\text{ex}} = 532$  nm) of a Q-switched Nd: YAG laser (NANO S120-20, Litron Lasers) operating at a repetition rate of 20 Hz and a pulse width of a 10 ns. The energy of laser was adjusted by using the calibrated neutral density filters. The pump beam was focused into a stripe whose shape was adjusted to  $2 \text{ mm} \times 0.03 \text{ mm}$  by using a 50 mm focal length cylindrical lens and an aperture. The emission was detected by a CCD-based fiber-probe Avantes spectrometer having a spectral resolution of 0.04 nm, coupled with a collection fiber of diameter 600  $\mu\text{m}$ . The optical waveguide property of the sample in unbent and bent shape was analysed by exciting at different sites of the crystal with a pump beam spot, which is having a width of 0.03 mm. The guided emission from the excited sample was collected from another end. The optical loss coefficient ( $\alpha$ ) was obtained by a single-exponential fitting of the function  $I_{\text{tip}}/I_{\text{body}} = A \exp(-\alpha D)$ , where  $I_{\text{tip}}$  and  $I_{\text{body}}$  are the fluorescence intensities of guided and incident light and  $D$  is the distance between the excited position and the end of the crystal for collecting emission.

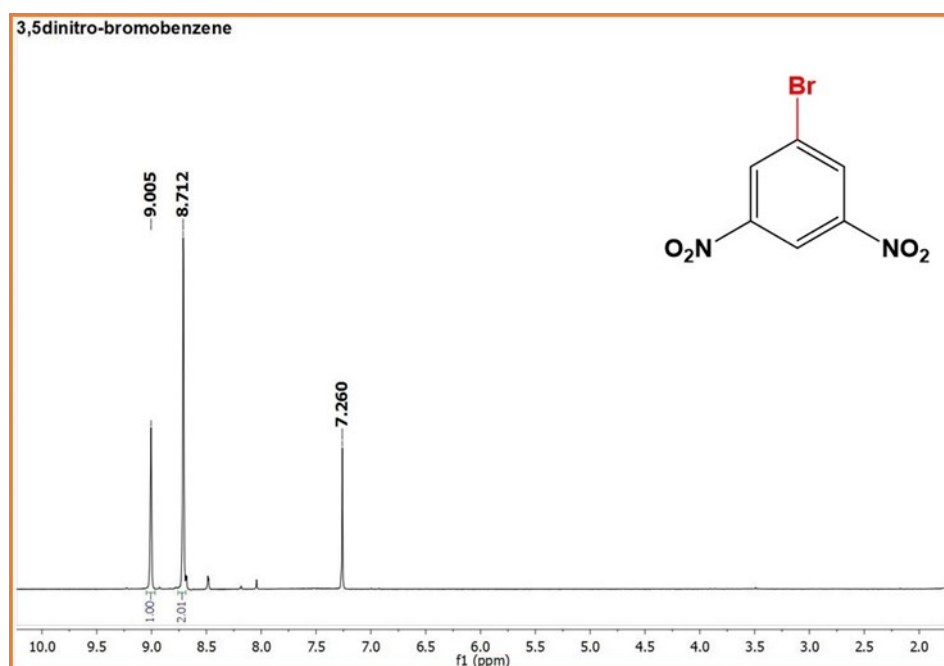
A schematic of the experimental setup used to study the optical properties of unbent and bent crystal is shown below. In which, L1, L2 represent convex lens; ND, neutral density filters; A, aperture; M, mirror; L3, cylindrical lens; TS, translational stage; S, sample; D, detector.



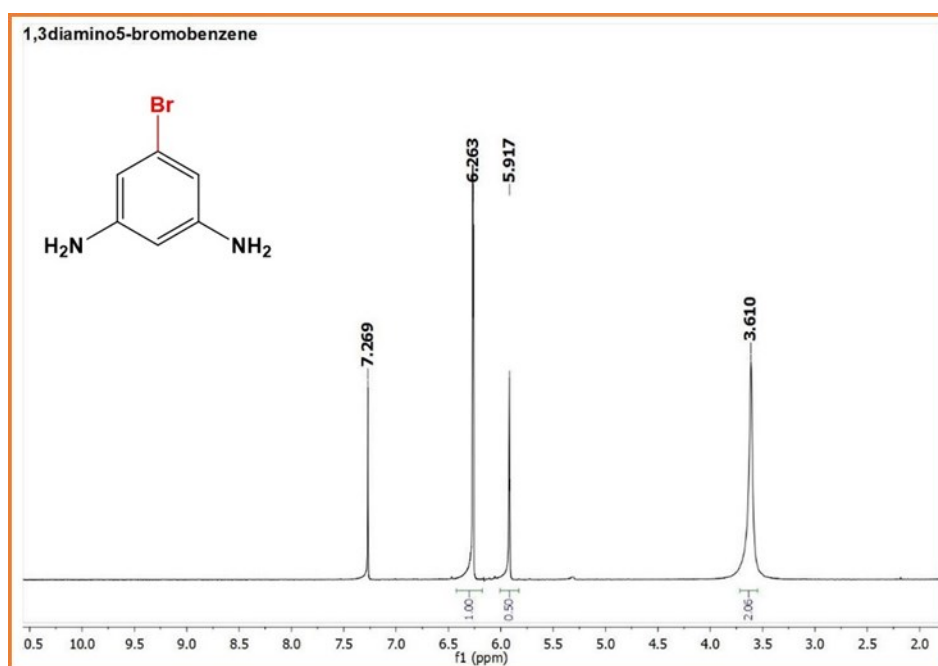
### Synthesis of compound 1:



**3,5-dinitro-1-bromobenzene:** 1,3 dinitrobenzene (2g, 0.011 mol) was taken in concentrated sulphuric acid (20 mL) and heated to 60 °C. To this solution N-bromosuccinimide (NBS) was added (0.022 mol, 3.91 g) in three portions each in 15 minutes. The reaction mixture was allowed to stir at 80 °C for 4h and poured into ice water. The precipitated solid was filtered and washed with water and recrystallized from methanol to obtain 3,5-dinitro-1-bromobenzene. Yield 95%.  $^1\text{H}$  NMR (400 MHz,  $\text{CDCl}_3$ )  $\delta$  9.0 (s, 1H), 8.71 (s, 2H).



**1,3-diamino-5-bromobenzene:** To a solution of 3,5-dinitrobromobenzene (2 g, 0.008 mol) in HCl was added an ethanolic solution of tin metal powder (2.84 g, 0.024 mol) in step wise for about 0.5 h and then subjected to stirring for 4h at 100 °C. After 4h, the entire reaction mixture was poured into cold water then neutralized with NaOH solution and then extracted into chloroform solution to obtain 1,3-diamino-5-bromobenzene. Yield 70%.  $^1\text{H}$  NMR (400 MHz,  $\text{CDCl}_3$ )  $\delta$  6.26 (s, 2H), 5.91 (s, 1H), 3.61 (s, 4H).



**1,3-diamino-2,4,5,6-tetrabromobenzene:**

To a solution of 1,3-diamino-5-bromobenzene (1 g, 0.005 mol) in chloroform, N-bromosuccinimide (NBS) was added (0.016 mol, 2.85 g) and allowed to stir for 5h at ambient temperature. The reaction mixture was poured into a beaker which contains  $\text{NaHCO}_3$  solution and allowed to stir for 10 minutes. The unreacted/side product of NBS was removed by discarding the aqueous solution. The same procedure is repeated for 3 to 4 times and then extracted from the organic layer, recrystallized from MeOH to obtain 1,3-diamino-2,4,5,6-tetrabromobenzene. Yield 65%.  $^1\text{H}$  NMR (400 MHz,  $\text{CDCl}_3$ )  $\delta$  4.75 (s, 4H).

1,3-diamino-2,4,5,6-tetrabromobenzene

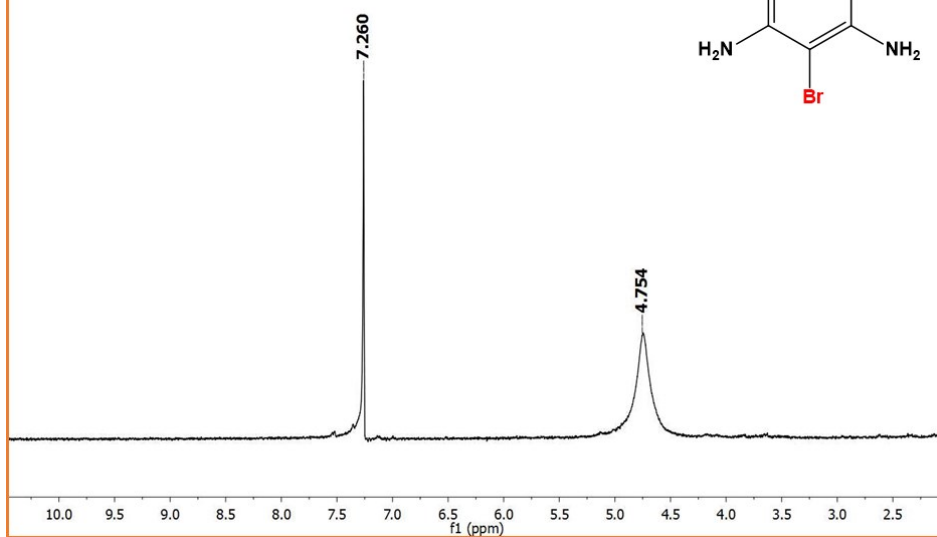


**Fig. S1:** Calculation of Elastic Strain

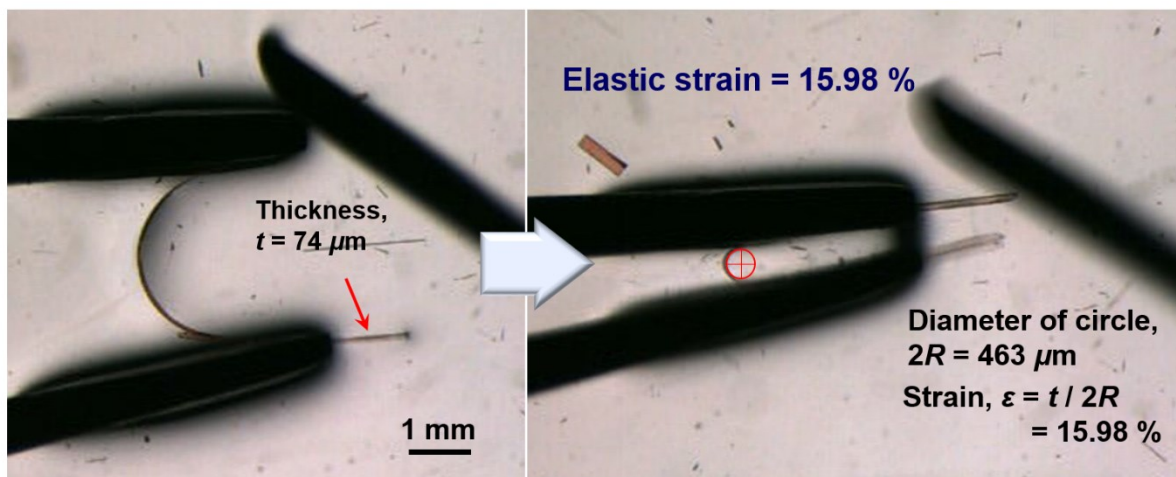
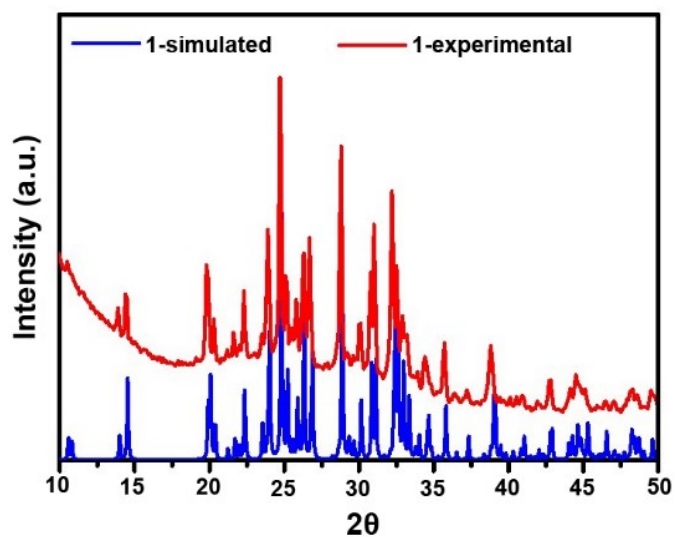


**Table S1:** Crystallographic parameters of compound **1**

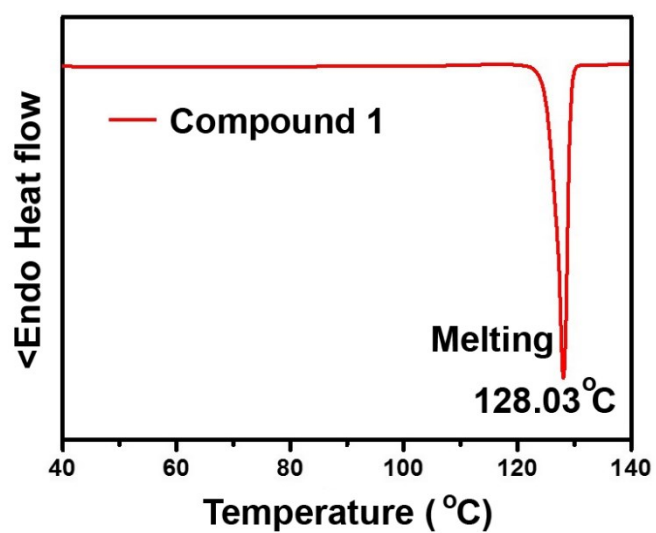
Crystal	<b>1</b>
Formula	C <sub>6</sub> H <sub>4</sub> Br <sub>4</sub> N <sub>2</sub>
Molecular weight	423.75
T(K)	296
Crystal system	Monoclinic
Space group	P2 <sub>1</sub> /c
a (Å)	14.1498 (12)
b (Å)	4.1793 (4)
c (Å)	17.4453 (16)
α (°)	90
β (°)	109.838 (3)
γ (°)	90
V (Å <sup>3</sup> )	970.43 (15)
Z	4
D <sub>cal</sub> (mg/m <sup>3</sup> )	2.9
R <sub>1</sub> [I > 2σ(I)]	0.0479
wR <sub>2</sub> (on F <sup>2</sup> , all data)	0.1542
CCDC Number	2077700



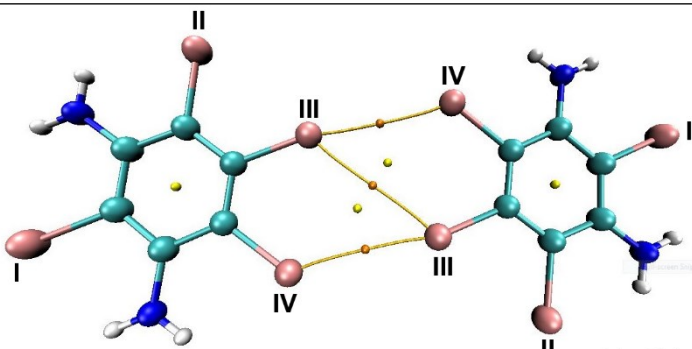
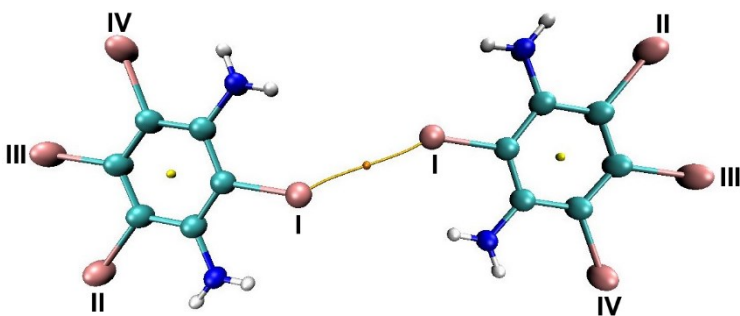
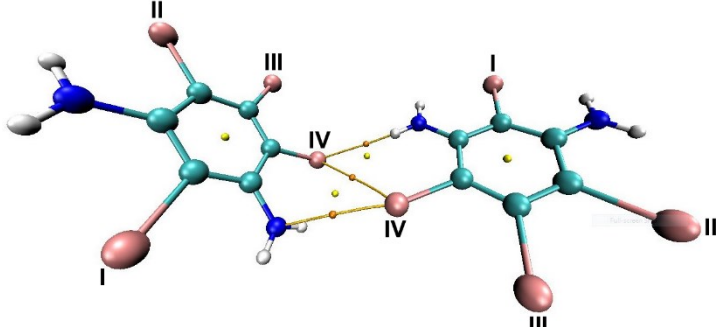
**Fig. S2:** An overlay of experimental and simulated powder X-ray diffraction pattern of compound 1



**Fig. S3:** DSC thermogram of compound 1



**Fig. S4:** QTAIM topology map to determine the halogen and hydrogen bond energies.

Compound 1	Interactions	Energy kcal/mol
	Br(III)⋯Br(IV)	-1.075
	Br(III)⋯Br(III)	-0.6548
	Br(I)⋯Br(I)	-0.985
	N-H⋯Br(IV)	-0.754
	Br(IV)⋯Br(IV)	-0.81
	C-N⋯Br(IV)	-1.24

**Fig. S5:** (a) Absorption and (b) emission spectra at 320 nm excitation of compound **1** in a range of non-polar to polar solvents.

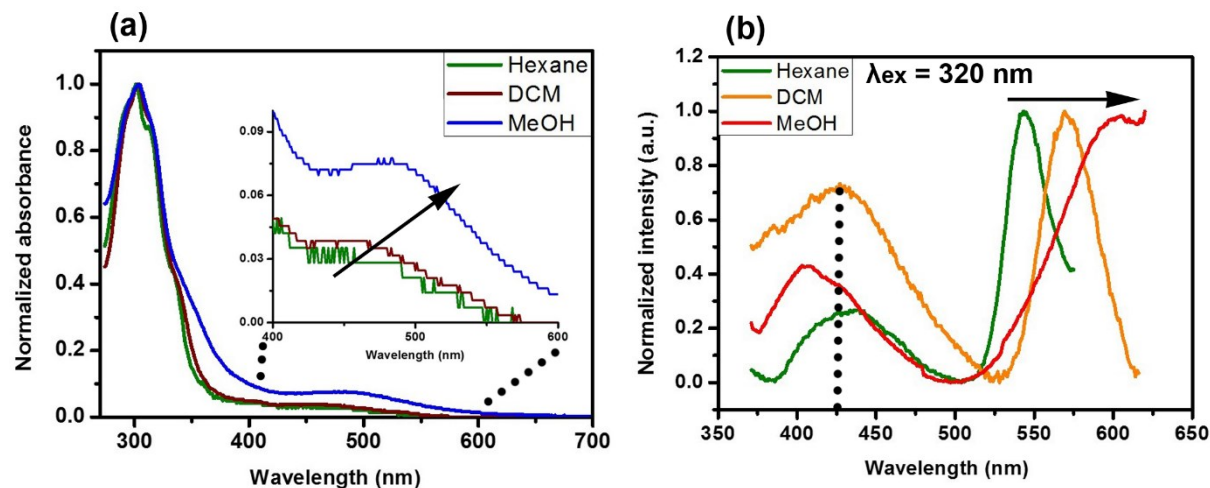


**Fig. S6:** Comparison of experimental absorption spectrum (a) solid and (b), (c) solution phase of compound **1** with the computed absorption spectrum at PBEPBE and DZVP level of theory. (d) Excitation spectra of compound **1** when emission was monitored at 590 nm.

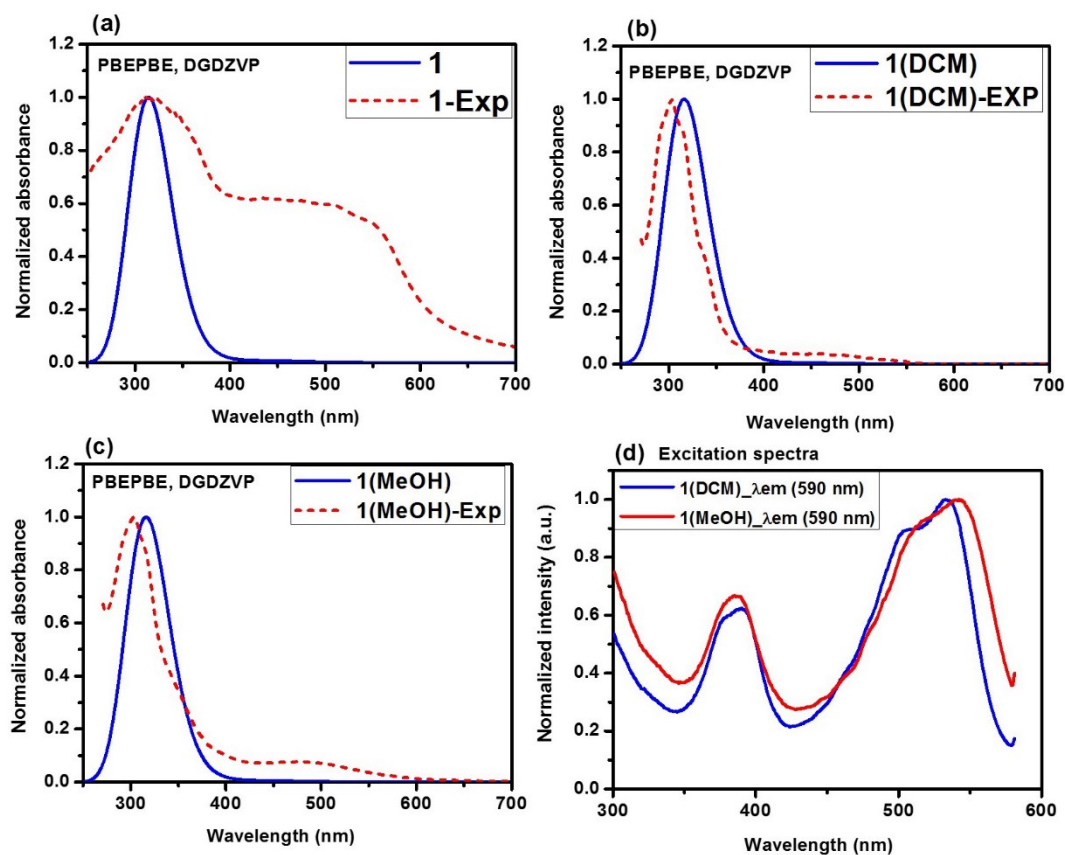


**Fig. S7:** The computed vertical excitation energies (VEEs) of compound **1** and nature transition orbitals (Iso value = 0.02) corresponding to various excited singlet states in vacuum at PBEPBE and DZVP level of theory. The “f” represents the oscillator strength of the transition.

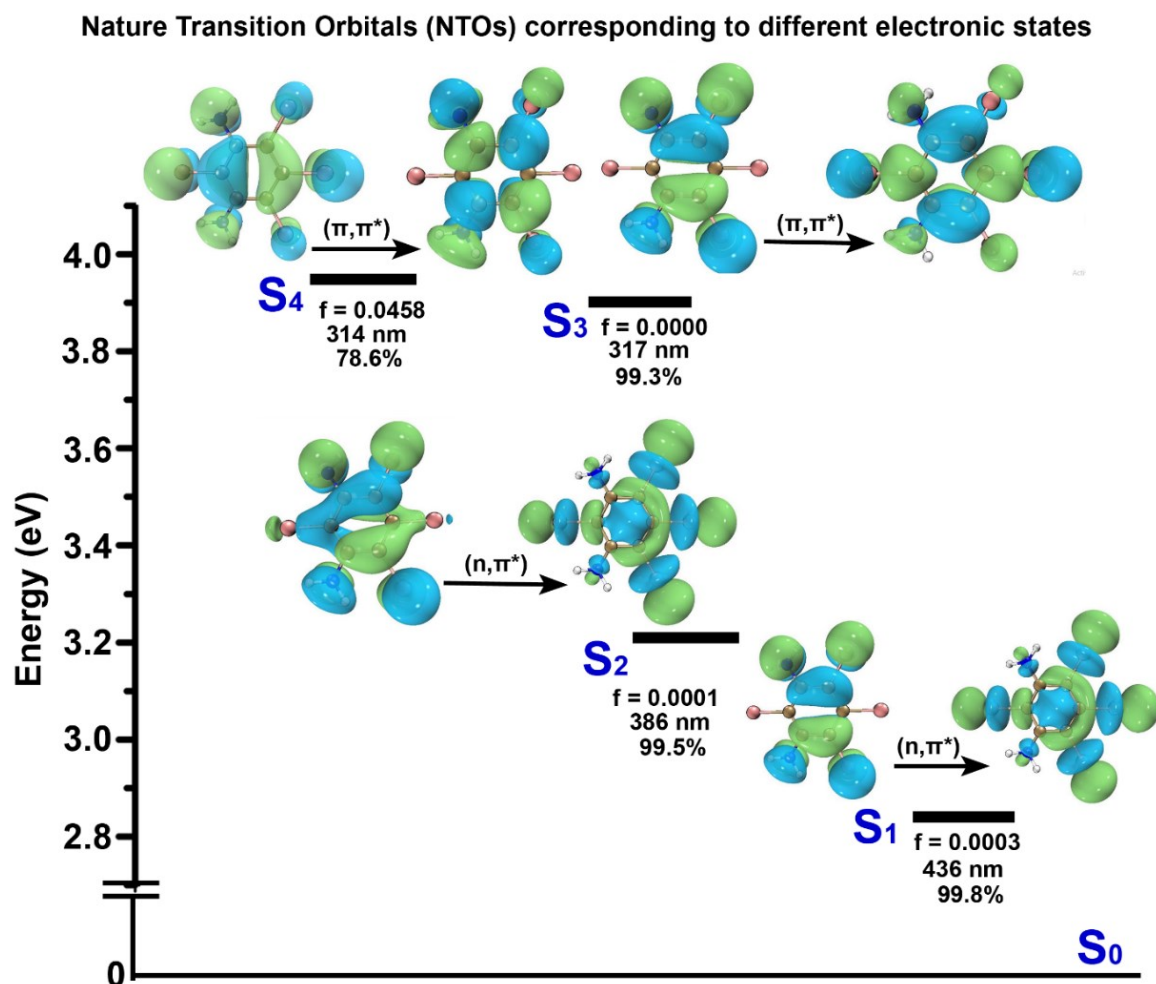


**Fig. S8:** The computed vertical excitation energies (VEEs) of compound **1** and nature transition orbitals (Iso value = 0.02) corresponding to various excited singlet states in dichloromethane at PBE/PBE and DZVP level of theory. The “f” represents the oscillator strength of the transition.

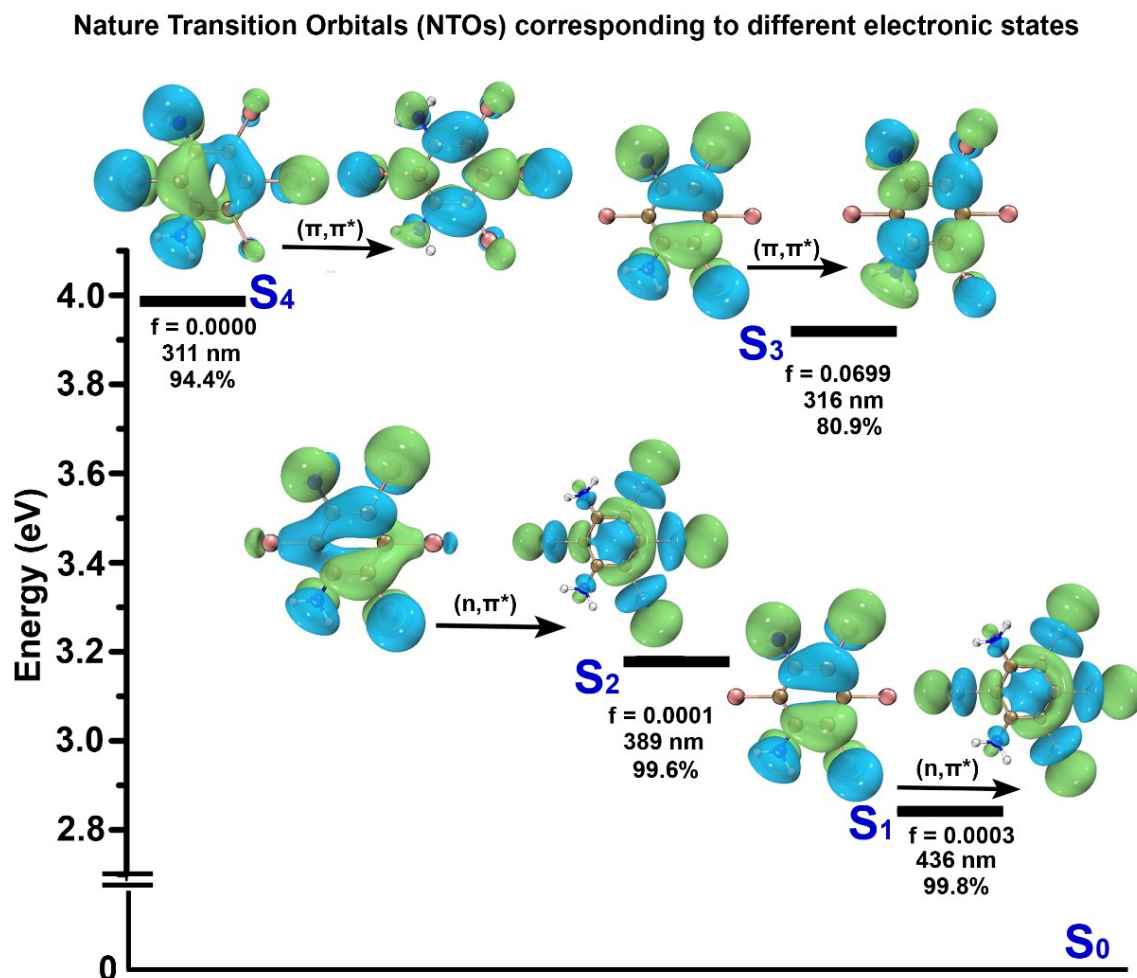


**Fig. S9:** Emission spectra of compound **1** crystal in (a) unbent (b) bent shape and (c) solid state

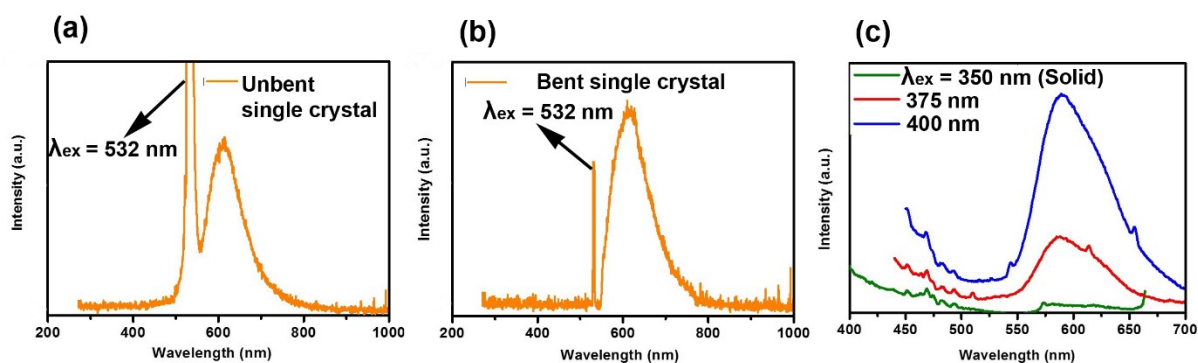


**Table S2:** Photo-physical parameters of compound **1**

Compound <b>1</b>	$\lambda_{\text{abs}}$ (nm)	$\lambda_{\text{em}}$ (nm)	$\Phi_{\text{F}}$	$\tau$ (ns)	$k_{\text{r}}$ ( $\times 10^8 \text{ s}^{-1}$ )	$k_{\text{nr}}$ ( $\times 10^8 \text{ s}^{-1}$ )	Goodness of fit ( $\chi^2$ )
DCM	315, 480	575	0.09	2.1 ( $\pm 0.01$ )	0.42	0.56	1.1
MeOH	315, 500	615	0.07	1.7 ( $\pm 0.01$ )	0.41	1.78	1.2

**Table S3:** The reported optical loss coefficient ( $\alpha$ ) of few organic single crystals and representative polymers.

Compound (organic single crystal/ representative polymer)	Shape of the crystal	Optical loss ( $\alpha$ ) coefficient (dB/mm)	Reference
Crystal 1	Unbent Bent (elastic)	0.043 0.047	Hayashi et al. <i>Angew. Chem. Int. Ed.</i> <b>2018</b> , 57, 17002-17008.
DMDAT	Unbent Bent (elastic) Bent (twisted)	0.145 0.144 0.144	Zhang et al. <i>Adv. Optical Mater.</i> <b>2019</b> , 7, 1900927.
Single benzene emitter	Unbent	0.26 (at 25 °C) 0.32 (at -95 °C)	Zhang et al. <i>Angew. Chem. Int. Ed.</i> <b>2020</b> , 59, 23117-23121.
1d@2d	Unbent Bent (elastic)	0.272 (at 576 nm) 0.196 (at 615 nm) 0.275 (at 576 nm) 0.192 (at 615 nm)	Zhang et al. <i>Adv. Mater.</i> <b>2018</b> , 30, 1800814.
DPIN	Unbent Bent (elastic)	0.27 0.274	Zhang et al. <i>Angew. Chem. Int. Ed.</i> <b>2018</b> , 57, 8448-8452.
BDTVA	Unbent	0.275	Tian et al. <i>ACS Photonics</i> <b>2015</b> , 2, 313-318.
DBBZL	Unbent Bent (elastic) Bent (plastic)	0.285 0.306 0.307	Zhang et al. <i>Chem. Sci.</i> , <b>2019</b> , 10, 227-232.
Polymorph A	Unbent Bent (elastic)	0.351 0.376	Zhang et al. <i>J. Phys. Chem. Lett.</i> <b>2019</b> , 10, 1437-1442.
CN-DPVB	Unbent Bent (elastic)	0.358 0.409	Zhang et al. <i>Angew. Chem. Int. Ed.</i> <b>2020</b> , 59, 4299-4303.

Compound 1	Unbent Bent (elastic)	0.69 0.99	Biradha et al. (This work)
DCA	Unbent  Bent (Plastic)	1.6 (at 530 nm) 1.2 (at 570 nm) 0.9 (at 610 nm) 1.9 (at 530 nm) 1.35 (at 570 nm) 0.65 (at 610 nm)	Naumov et al. <i>Angew. Chem. Int. Ed.</i> <b>2018</b> , 57, 17254-17258.
ZnCl <sub>2</sub> -B (micro/nanorod)	Unbent	1 (at 375 nm); 2 (at 488 nm); 7 (at 405 nm)	Yan et al. <i>Adv. Mater.</i> <b>2021</b> , 33, 2007571.
BCPEB	Unbent	3	Xu et al. <i>J. Mater. Chem.</i> , <b>2012</b> , 22, 1592-1597.
PyB	Unbent	3.51 (at 497 nm) 6.69 (at 440 nm)	Jia et al. <i>ACS Appl. Mater. Interfaces</i> <b>2017</b> , 9, 8910-8918.
DCA	Unbent	5.8	Cui et al. <i>Mater. Chem. Front.</i> , <b>2018</b> , 2, 910-916.
CHICZ	Unbent	10 (along) 20 (perpendicular)	Hu et al. <i>Nat. Commun.</i> <b>2018</b> , 9, 4790.
C1 C2 C3	Unbent Bent (elastic) Unbent Bent (elastic) Unbent Bent (elastic)	9.43 9.37 28.02 25.95 11.71 13.24	Chandrasekar et al. <i>Angew. Chem. Int. Ed.</i> <b>2020</b> , 59, 13821-13830.
DPEpe-F4DIB Microtube	Unbent	14.5	Zhuo et al. <i>J. Mater. Chem. C</i> , <b>2018</b> , 6, 9594-9598.
DPEpe-F4DIB microrod	Unbent	34.1	
3TBT	Unbent	36	Motamen et al. <i>Phys. Chem. Chem. Phys.</i> , <b>2017</b> , 19, 15980-15987.
NVP-THA	Unbent	66	Yan et al. <i>Angew. Chem. Int. Ed.</i> <b>2020</b> , 59, 22623-22630.
2PL	Unbent	120	Chandrasekar et al. <i>Adv. Optical Mater.</i> <b>2019</b> , 7, 1801775.
PDI microwires	Unbent	130	Bao et al. <i>Adv. Mater.</i> <b>2010</b> , 22, 3661-3666.
TPE-HPh-Bar	Unbent	137	Wang et al. <i>J. Mater. Chem. C</i> , <b>2014</b> , 2, 1801-1807.

F8BT	---	0.76	Xia et al. <i>Appl. Phys. Lett.</i> <b>2003</b> , 82, 3599.
F8DP	---	1.48	Xia et al. <i>Appl. Phys. Lett.</i> <b>2003</b> , 82, 3599.
DOO-PPV	---	3	Frolov et al. <i>Phys. Rev. B</i> <b>1998</b> , 57, 9141.
BuEH-PPV	---	4.4	McGehee et al. <i>Phys. Rev. B</i> <b>1998</b> , 58, 7035.

## References:

1. G. M. Sheldrick, SHELXL-2014; University of Göttingen and Bruker AXS: Karlsruhe, 2014.
2. M. J. Frisch, G. W. Trucks, H. B. Schlegel, G. E. Scuseria, M. A. Robb, J. R. Cheeseman, G. Scalmani, V. Barone, B. Mennucci, G. A. Petersson, H. Nakatsuji, M. Caricato, X. Li, H. P. Hratchian, A. F. Izmaylov, J. Bloino, G. Zheng, J. L. Sonnenberg, M. Hada, M. Ehara, K. Toyota, R. Fukuda, J. Hasegawa, M. Ishida, T. Nakajima, Y. Honda, O. Kitao, H. Nakai, T. Vreven, J. A. Montgomery Jr, J. E. Peralta, F. Ogliaro, M. Bearpark, J. J. Heyd, E. Brothers, K. N. Kudin, V. N. Staroverov, R. Kobayashi, J. Normand, K. Raghavachari, A. Rendell, J. C. Burant, S. S. Iyengar, J. Tomasi, M. Cossi, N. Rega, N. J. Millam, M. Klene, J. E. Knox, J. B. Cross, V. Bakken, C. Adamo, J. Jaramillo, R. Gomperts, R. E. Stratmann, O. Yazyev, A. J. Austin, R. Cammi, C. Pomelli, J. W. Ochterski, R. L. Martin, K. Morokuma, V. G. Zakrzewski, G. A. Voth, P. Salvador, J. J. Dannenberg, S. Dapprich, A. D. Daniels, Ö. Farkas, J. B. Foresman, J. V. Ortiz, J. Cioslowski, and D. J. Fox, Gaussian 09, Revision A.1; Gaussian Inc.: Wallingford, CT, 2009.
3. Dey, S.; Das, S.; Bhunia, S.; Chowdhury, R.; Mondal, A.; Bhattacharya, B.; Devarapalli, R.; Yasuda, N.; Moriwaki, T.; Mandal, K.; Mukherjee, G. D.; Reddy, C. M. Mechanically interlocked architecture aids an ultrastiff and ultra-hard elastically bendable cocrystal. *Nature Commun.* **2019**, 10, 3711.
4. Devarapalli, R.; Kadambi, S. B.; Chen, C. T.; Gamidi, R. K.; Kammari, B. R.; Buehler, M. J.; Ramamurty, U.; Reddy, C. M. Remarkably Distinct Mechanical Flexibility in Three Structurally Similar Semiconducting Organic Crystals Studied by Nanoindentation and Molecular Dynamics. *Chem. Mater.* **2019**, 31, 1391-1402.